Journal of Information Display
Vol. 12, No. 1, March 2011, 11–15

Taylor & Francis
Taylor & Francis Group

High-brightness and wide-view transflective liquid crystal display with two in-cell imprinted optical films in an inverse-twisted-nematic geometry

Jun-Hee Na[a], Seong-Min Cho[a], Sin-Doo Lee[a]* and Yong-Woon Lim[b]

[a] *School of Electrical Engineering, #032, Seoul National University, Kwanak, P.O. Box 34, Seoul 151-600, South Korea;* [b] *LCD Business, Samsung Electronics Co., Ltd., San #24 Nongseo-dong, Giheung-gu, Yongin City, Gyoenggi-do 446-711, South Korea*

(*Received 27 September 2010; Revised 19 November 2010; Accepted for publication 19 November 2010*)

An inverse-twisted-nematic (ITN) transflective (TRF) liquid crystal (LC) display, where two imprinted optical films (IOFs) with surface microstructures are embedded was developed. One of the IOFs serves as an in-cell patterned retarder with multi-optic axes, and the other behaves as a viewing-angle enhancement film. In the presence of an applied voltage, the surface microstructures on the IOFs provide the spontaneous twist of the LC from a vertically aligned state to a 90° twisted-nematic (TN) state in the transmissive part, and to a 45° TN state in the reflective part. The developed ITN TRF LC display exhibits high transmission and reflectance, fast response, and wide-viewing characteristics, along with achromaticity.

Keywords: wide-viewing; transflective; inverse twisted nematic; imprinted optical film; achromaticity

1. Introduction

The importance of transflective (TRF) liquid crystal displays (LCDs) has increased tremendously for mobile applications because of their low power consumption and excellent outdoor readability. The individual pixels in the TRF LCD are usually divided into two parts: the transmissive (T) and reflective (R) parts [1,2]. Backlight passes once through the LC layer in the T part, while ambient light traverses the LC layer twice in the R part. Therefore, an optical-path difference (OPD) between the two parts inevitably appears, and it should be compensated by an electro-optic (EO) effect in either a dual- or single-cell gap configuration [3,4]. Several LC modes, such as the conventional twisted-nematic (TN) mode and the in-plane switching and vertically aligned (VA) modes, have been employed to fabricate the TRF LCDs, some of which still suffer from narrow-viewing properties, low luminance, or limited contrast ratio [5–7]. In this work, a wide-viewing TRF LC cell with high optical efficiency consisting of two imprinted optical films (IOFs) in an inverse-twisted-nematic (ITN) geometry was demonstrated. The two IOFs were made of a liquid crystalline polymer (LCP), one of which served as an in-cell patterned retarder with multi-optic axes in the lower glass substrate, and the other as a viewing-angle enhancement film in the upper glass substrate [8,9]. For uniform alignment, the LCP films were patterned using an imprinting technique with a silane-treated polymer mold [10]. The embedded microstructures of such IOFs enable the alignment of the LCs due to the Berreman topographical effect [11], and the patterns with multi-optic axes are capable of compensating the OPD between the T and R parts. It was found that the TRF LC cell in an ITN geometry exhibits high optical efficiency, wide-viewing properties, and achromaticity.

2. Experimental considerations

The schematic diagram in Figure 1 shows the operation principle of the developed TRF LC cell using the ITN mode in a single-cell gap configuration. Two IOFs with microstructures were placed on the inner surfaces of indium-tin-oxide glass substrates. One of the IOFs on the lower substrate served as a patterned retarder (a positive A plate: $n_x > n_y = n_z$) with binary patterns the directions of which were 45° and 0° with respect to one of two polarizers, respectively [8]. Here, n_x, n_y, and n_z were refractive indices of the x, y, and z axes, respectively. The other IOF on the upper substrate behaved as a viewing-angle enhancement film of a positive C plate ($n_z > n_x = n_y$) with only one type of pattern. A nematic LC material with negative dielectric anisotropy was injected into the developed cell via capillary action in the isotropic state. Note that fluorosilane treatment was conducted to avoid strong adhesion for high-resolution microstructures on the surface of the IOF, and to induce the spontaneous homeotropic alignment of the LC molecules [12]. In the absence of an applied voltage, the LC molecules were VA in the T and R parts, as shown in Figure 1(a), and no phase difference between the T and R parts appeared.

*Corresponding author. Email: sidlee@plaza.snu.ac.kr

ISSN 1598-0316 print/ISSN 2158-1606 online

DOI: 10.1080/15980316.2011.555509
http://www.informaworld.com

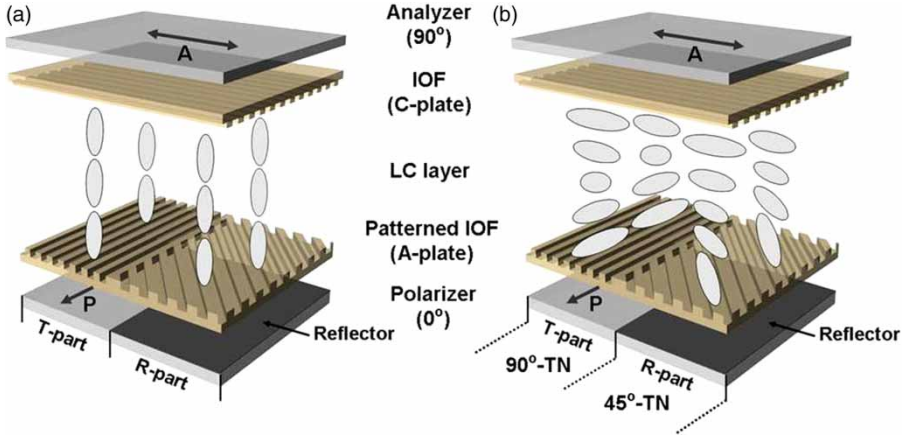

Figure 1. Schematic diagram showing the operation principle of the developed ITN TRF LC cell: (a) under no applied voltage (a dark state) and (b) in the presence of an applied voltage (a bright state).

In the T part, the linearly polarized light passed through the positive A plate and the LC cell without a phase change. Therefore, the incident light did not experience any birefringence, and the initial polarization state was maintained. Thus, under crossed polarizers, no light propagates, and a completely dark state is obtained. Note that the positive A plate in the T part acts as a dummy layer as the A plate and the transmitted light through the lower polarizer have the same optic axes. In the R part, the incident light passes through both the A plate with a phase retardation like a quarter-wave plate (QWP), and the LC layer with no phase retardation, so that the linearly polarized light is converted into a circularly polarized light. This light is reflected from a metal reflector, is linearly polarized by the QWP, and is completely blocked by the upper polarizer. In the presence of an applied voltage, the LC layer assumes a 90° TN state in the T part and a 45° TN state in the R part due to the homeotropic-to-twisted-planar transition [13]. In the T part, the linearly polarized light passing through the 90° TN LC layer has a wave-guiding effect, and a bright state is then obtained. In the R part, the linearly polarized state of ambient light is rotated by $+45°$ through the LC layer and then by $-45°$ upon reflection from the mirror. Accordingly, a bright state is achieved. Note that the positive C plate placed inside the upper substrate produced no optical modulation in the R part.

3. Results and discussion

For TRF LCDs with less optical-efficiency loss in both the T and R parts, the introduction of a QWP is desirable inside the LC cell [14]. In these authors' previous research work [8], such in-cell QWP was fabricated using an imprinting technique. Figure 2 shows microscopic textures and the corresponding phase retardation values of a positive C plate and a patterned positive A plate. The two IOFs were made of two LCPs: RMS03-015 (E. Merck) and RMS03-001C (E. Merck). As shown in Figure 2(a) and (b), the imprinted RMS03-015 film always shows a dark state irrespective of the rotation angle under the crossed polarizers because the LCP molecules were aligned vertically. This C plate can be used as a viewing-angle enhancement film. The homeotropically aligned LCP molecules were spontaneously produced using the hydrophobic surface property of the polymer mold of poly(dimethylsiloxane) (PDMS, GE Silicones). On the other hand, the IOF of RMS03-001C, placed on the bottom substrate, has the optical symmetry of a positive A plate with two optic axes in the planar alignment. Binary patterns the directions of which make up an angle of 45° to each other were produced using a predefined polymer mold through the imprinting process. One type of binary pattern in the patterned A plate is dark, and the other is white, when the optic axis coincides with one of the two crossed polarizers, as shown in Figure 2(c) and (d). When the patterned A plate is rotated under the crossed polarizers, the two patterns switch between a dark state and a bright state. Figure 2(e) shows the values of the phase retardation, $2\pi d\Delta n/\lambda$, of the patterned A plate, measured as a function of the azimuthal angle using a photoelastic modulation technique (PEM, Hinds Instrument, Inc.) [15]. Here, d, Δn, and λ represent the film thickness, the birefringence of the film, and the wavelength of the light source used, respectively. As a light source, a 632.8 nm He–Ne laser was used to measure the EO properties of the developed TRF LC cell. All the measurements were carried out at room temperature. The maximum phase retardation values of the binary patterns in the A plate at the angles of 0° and 45° with respect to the polarizer were about 1.6, which correspond to the value of a QWP at the wavelength of $\lambda = 632.8$ nm. Note that the microstructure patterns produced on the surfaces of the two IOFs (the C and A plates) are capable of spontaneously aligning the LC molecules without an additional treatment, such as the polyimide-coating process. The azimuthal anchoring energy measured using the cell

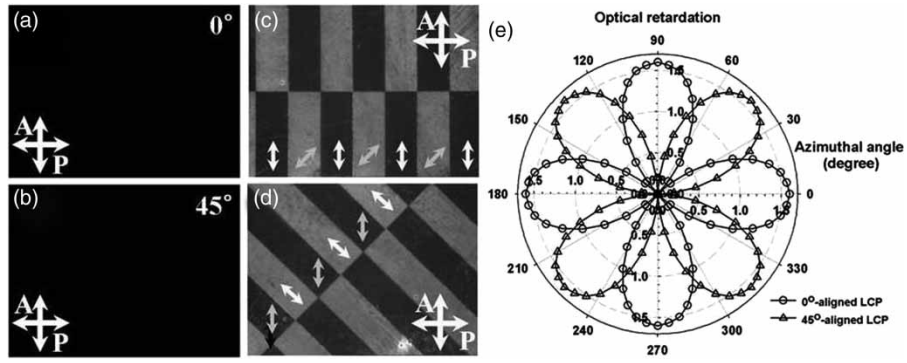

Figure 2. The microscopic textures of the IOFs behaving as a positive C plate and as a patterned positive A plate, which were observed under crossed polarizers. The C plate is always dark irrespective of the rotation angles (a) 0° and (b) 45° with respect to the polarizer. The two directions of the binary patterns in the A plate were (c) 0° and (d) 45° with respect to the polarizer, and the phase retardation values of the two domains in the patterned A plate measured as a function of the azimuthal angle were in (e). The symbols P and A represent the polarizer and analyzer, respectively.

rotation method was found to be about $8.43 \times 10^{-6}\,\mathrm{J/m^2}$ [15], which is in the strong anchoring regime.

The nematic LC material that was used in this work was MJ-96758 (E. Merck). The material parameters of MJ-96758 that were used for the numerical simulations via the relaxation method [16] were the three elastic constants $K_1 = 13.0\,\mathrm{pN}$, $K_2 = 7.0\,\mathrm{pN}$, and $K_3 = 15.0\,\mathrm{pN}$, the dielectric anisotropy $\Delta\varepsilon = -4.9$, and the rotational viscosity $\gamma = 0.148\,\mathrm{Pa\,s}$. The ordinary and extraordinary refractive indices were $n_o = 1.4582 + 5558/\lambda^2$ and $n_e = 1.5323 + 7784/\lambda^2$, respectively. Here, λ is the wavelength of the incident light in the nanometer. The cell gap was maintained using 4-μm-thick glass spacers.

The EO characteristics and the dynamic response in both the T and R parts were first examined. Figure 3(a) shows the experimental and numerical simulation results for the EO properties of the developed TRF LC cell as a function of the applied voltage. The ratios of the output intensity to the input intensity in the T and R parts were 0.42 and 0.41, respectively. The data denoted by the two symbols are the experimental results, and the solid lines represent the numerical simulation results. The experimental data well coincide with the simulation results, as shown in Figure 3(a). Except for the slope of the EO curve, the threshold behavior and saturated light intensity in the T and R parts are quite similar. This allows the operation of the TRF LC cell in a rather simple driving scheme. Figure 3(b) shows the EO dynamic response of the developed TRF LC cell to a bipolar applied voltage in a square-wave form of 5 V at 1 kHz in both the R and T parts. The rising and falling times, determined from the normalized EO response, were about $\tau_{on} = 5.2\,\mathrm{ms}$ and $\tau_{off} = 18.1\,\mathrm{ms}$, respectively. This switching speed range will be further improved using a fast response LC material for high-speed applications.

The isocontrast contours, measured using a spatial photometer (EZ Contrast 160R, ELDIM), of two TRF LC cells,

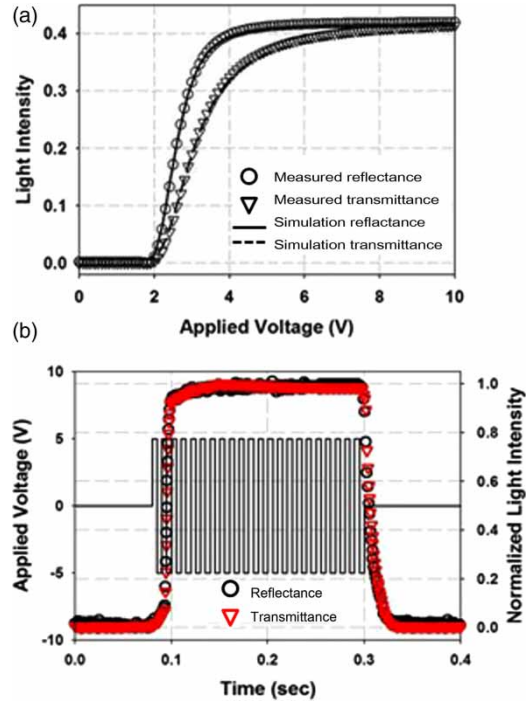

Figure 3. The EO characteristics of the developed TRF ITN LC cell: (a) Transmittance and reflectance as functions of an applied voltage in square-wave form. (b) The dynamic EO response properties. The open circles and inverted triangles denote the experiment results of the EO properties in the R and T parts, respectively. The solid lines in (a) represent the numerical simulation results.

one of which has only a patterned plate A and the other both patterned A and C plates, will now be shown. As shown in Figure 4(a) and (b) in the T and R parts, it is clear that the viewing angle is substantially enhanced by the C plate placed on the upper substrate compared to Figure 4(c) and (d), where no C plate was used. The T part shows a contrast ratio $> 10:1$ on a more-than-60° viewing cone

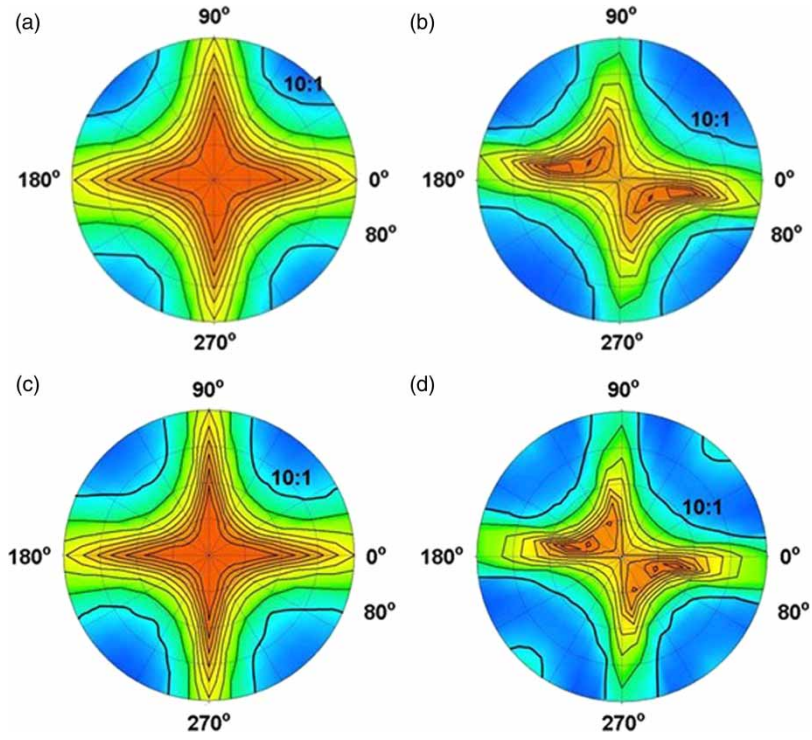

Figure 4. Isocontrast contours in the (a) T part and (b) R part of the developed TRF ITN LC cell with the C plate compared with those in the (c) T part and (d) R part of the TRF ITN LC cell with no C plate.

in all directions, as shown in Figure 4(a). The viewing properties are quite symmetric with respect to the polarizer direction. In the R part, they are quite asymmetric, and the contrast ratio is somewhat lower than that in the T part. The C plate has the important role of effectively enhancing the viewing angle by at least 10° in the developed TRF LC cell.

4. Conclusion

A wide-viewing TRF LCD in an ITN configuration and with a single-cell gap was demonstrated. The OPD between the T and R parts were well compensated using the patterned A plate of the IOF, which was made of aligned LCP molecules. The use of the C plate inside the TRF LCD cell was found to produce enhanced viewing properties. Moreover, the IOFs with single or binary microstructure patterns were found to be capable of spontaneously aligning the LC molecules without any additional surface treatment. The TRF LC cell with the IOFs presented here shows an analog grayscale capability with the good linearity, fast response, and high transmission and reflectance required for displaying dynamic images.

Acknowledgements

This work was supported in part by Samsung Mobile Display Co., Ltd. and Inter-University Semiconductor Research Center (ISRC) of Seoul National University.

References

[1] X. Zhu, Z. Ge, T.X. Wu, and S.-T. Wu, J. Disp. Technol. **1**, 15 (2005).
[2] D.-W. Kim, J.-H. Na, J.-H. Hong, and S.-D. Lee, Jpn. J. Appl. Lett. **48**, 090204 (2009).
[3] T.-J. Chen and K.-L. Chu, Appl. Phys. Lett. **92**, 091102 (2008).
[4] E.J. Jeon, S.S. Kim, Y.J. Lim, E.M. Jo, Y.J. Choi, M.-H. Lee, T.J. Chung, and S.H. Lee, International Display Research Conference (2008), p. 141.
[5] H.-I. Baek, Y.-B. Kim, K.-S. Ha, D.-G. Kim, and S.-B. Kwon, Proc. 7th Int'l Display Workshops (Soc. Inf. Dis., Kobe, 2000), p. 41.
[6] R. Lu, Z. Ge, Q. Hong, and S.-T. Wu, J. Disp. Technol. **3**, 15 (2007).
[7] Y.-J. Lee, T.-H. Lee, J.-W. Jung, H.-R. Kim, Y. Choi, S.-G. Kang, Y.-C. Yang, S. Shin, and J.-H. Kim, Jpn. J. Appl. Phys. **45**, 7827 (2006).
[8] Y.-W. Lim, C.-H. Kwak, and S.-D. Lee, J. Nanosci. Nanotechnol. **8**, 4775 (2008).
[9] Y.-W. Lim, D.-W. Kim, and S.-D. Lee, Mol. Cryst. Liq. Cryst. **489**, 183 (2008).
[10] S.Y. Chou, P.R. Krauss, and P.J. Renstrom, Appl. Phys. Lett. **67**, 3114 (1995).
[11] D.W. Berreman, Phys. Rev. Lett. **28**, 1683 (1972).
[12] Y.S. Kim, N.Y. Lee, J.R. Lim, M.J. Lee, and S. Park, Chem. Mater. **17**, 5867 (2005).
[13] S.-W. Suh, S.T. Shin, and S.-D. Lee, Appl. Phys. Lett. **68**, 2819 (1996).

[14] S.-T. Wu, D.-K. Yang, *Reactive Liquid Crystal Displays* (Wiley, New York, 2001).

[15] J.-H. Lee, C.-J. Yu, and S.-D. Lee, Mol. Cryst. Liq. Cryst. **321**, 317 (1998).

[16] See, for example, W.H. Press, B.P. Flannery, S.A. Teukolsky, and W.T. Vetterling, *Numerical Recipes: The Art of Scientific Computing* (Cambridge University Press, Cambridge, 1986).